Optimization of continuous astaxanthin production by Haematococcus pluvialis in nitrogen-limited photobioreactor

Khadija Samhat, Antoinette Kazbar, Hosni Takache, Olivier Gonçalves, Delphine Drouin, Ali Ismail, Jeremy Pruvost

Algal Research 80 (2024) 103529

Contents lists available at ScienceDirect

Algal Research

journal homepage: www.elsevier.com/locate/algal

Optimization of continuous astaxanthin production by *Haematococcus pluvialis* in nitrogen-limited photobioreactor

Khadija Samhat [a,b], Antoinette Kazbar [c,d], Hosni Takache [e], Olivier Gonçalves [a], Delphine Drouin [a], Ali Ismail [b], Jeremy Pruvost [a,*]

[a] Nantes University, Oniris, CNRS, GEPEA, UMR 6144, F-44600 Saint-Nazaire, France
[b] Lebanese University, Platform for Research and Analysis in Environmental Sciences, Doctoral School of Science and Technology, Rafik Hariri Campus, Beirut, Lebanon
[c] Algosource, 7 Rue Eugène Cornet, F-44600 Saint-Nazaire, France
[d] Bioprocess Engineering, Wageningen University and Research, Wageningen, Netherlands
[e] Bio-Information Research Laboratory (BIRL), The Higher Institute of Biotechnologies of Paris (Sup'biotech), 66 rue Guy Môquet, 94800 Villejuif, France

ARTICLE INFO

Keywords:
Haematococcus pluvialis
Photobioreactor
Astaxanthin productivity
Continuous cultivation
Nitrogen limitation
Light transfer

ABSTRACT

The industrial production of astaxanthin from *Haematococcus pluvialis* is mainly operated following a two-stage cultivation strategy in photobioreactors (PBRs) operating in batch mode. This study provides a strategy for optimizing continuous astaxanthin production in a one-stage approach, by optimizing both astaxanthin accumulation and biomass productivity of *H. pluvialis* under nitrogen-limited condition. To achieve the good balance in culture conditions to maintain growth under nitrogen-limited conditions, while triggering significant astaxanthin accumulation in reddish vegetative cells, the role of light absorption, as represented by the mean rate of photon absorption (MRPA), and nitrate concentration was especially investigated. For that purpose, *H. pluvialis* cultures were grown in a flat-panel PBR with constant dilution rate D of 0.015 h^{-1}, different photon flux densities PFDs ranging from 75 to 750 $\mu mol_{h\nu} \cdot m^{-2} \cdot s^{-1}$ and different nitrogen concentration levels in the feeding medium [NO_3^-] of 1, 3 and 8.8 mM. A parabolic relationship between MRPA and astaxanthin production rate was obtained. This indicated that astaxanthin synthesis was limited by the MRPA, opening further optimization by adjusting incident light intensity, nitrogen concentration in the feeding medium or culture dilution rate. After optimization of operating conditions, we demonstrated that a large quantity of astaxanthin can be produced in continuous mode, following then a one-stage strategy which may be advantageous for industrial use. A maximum astaxanthin productivity of 1.27 ± 0.03 $g \cdot m^{-2} \cdot d^{-1}$ with an astaxanthin accumulation of 3.9 ± 0.2 % DW was reached for the culture featuring MRPA of 9000 $\mu mol_{h\nu} \cdot kg_x^{-1} \cdot s^{-1}$. The process was also proved reversible, allowing to tailor the biomass composition and physiological state (from green to red cells enriched in astaxanthin) by adjusting operating conditions, opening perspectives from an optimized coupling with downstream processing steps.

1. Introduction

Microalgae are commercially important for the food industry and aquaculture as a natural source of high-value products such as carotenoids, fatty acids, steroids, and polysaccharides [1,2]. Among the commercially important microalgae, *Haematococcus pluvialis*, also referred to as *Haematococcus lacustris*, is the richest and most promising source of natural astaxanthin, a carotenoid known for its antioxidant and coloring properties with already existing applications in nutraceuticals, cosmetics, food and aquaculture industries [3–5]. Astaxanthin antioxidant activity is around 10 times higher than other carotenoids such as β-carotene and lutein, and over 500 times higher than α-tocopherol [3,4]. Moreover, natural astaxanthin as issued from *H. pluvialis* has a significantly higher antioxidant capacity than synthetic one [6,7]. It was reported that *H. pluvialis* can accumulate large amounts of astaxanthin (up to 4–5 % DW) depending on the cultivation conditions and photobioreactor (PBR) design [8–13].

H. pluvialis is a unicellular, eukaryotic, green microalga. It is found naturally in fresh water. It has a slow growth rate and a complex life cycle with three common morphotypes observed: green flagellated macrozoïd, non-motile palmelloïd and red aplanospore [11]. The largest

* Corresponding author.
E-mail address: jeremy.pruvost@univ-nantes.fr (J. Pruvost).

https://doi.org/10.1016/j.algal.2024.103529
Received 5 December 2023; Received in revised form 15 April 2024; Accepted 29 April 2024
Available online 1 May 2024

Nomenclature

$<\mathscr{A}>$	mean rate of photon absorption[$\mu mol_{h\nu} \cdot kg_x^{-1} \cdot s^{-1}$]
$\mathscr{A}(z)$	local rate of photon absorption[$\mu mol_{h\nu} \cdot kg_x^{-1} \cdot s^{-1}$]
$A_{abs,\lambda}$	spectral mass absorption cross-section[$m^2 \cdot kg^{-1}$]
$\overline{A}_{abs,\lambda}$	average mass absorption cross-section[$m^2 \cdot kg^{-1}$]
a_{light}	specific illuminated surface of the PBR[m^{-1}]
C_{asta}	astaxanthin concentration[$g \cdot m^{-3}$]
$C_{Chl\text{-}a}$	chlorophyll *a* concentration[$g \cdot m^{-3}$]
$C_{Chl\text{-}b}$	chlorophyll *b* concentration[$g \cdot m^{-3}$]
C_x	biomass concentration[$kg \cdot m^{-3}$]
D	culture dilution rate[h^{-1}]
f_{asta}	astaxanthin fraction[total carotenoids %]
$G_\lambda(z)$	spectral fluence rate[$\mu mol_{h\nu} \cdot m^{-2} \cdot s^{-1}$]
L	thickness of the PBR[m]
P_{asta}	volumetric astaxanthin productivity[$g \cdot m^{-3} \cdot d^{-1}$]
PFD	photon flux density[$\mu mol_{h\nu} \cdot m^{-2} \cdot s^{-1}$]
P_x	volumetric biomass productivity[$g \cdot m^{-3} \cdot d^{-1}$]
$R_{nh,\lambda}$	normal-hemispherical reflectance[dimensionless]
SNI	specific nitrate input[$mg_{\overline{NO3}} \cdot g_x^{-1} \cdot d^{-1}$]
S_{asta}	areal astaxanthin productivity[$g \cdot m^{-2} \cdot d^{-1}$]
S_{light}	illuminated area of the PBR[m^2]
S_x	areal biomass productivity[$g \cdot m^{-2} \cdot d^{-1}$]
$T_{nh,\lambda}$	normal-hemispherical transmittance[dimensionless]
V_r	working volume of the PBR[m^3]
W_{asta}	astaxanthin content[DW %]
W_{chl}	chlorophyll content[DW %]
$Y_{NO_3^-/x}$	nitrate uptake yield[$mg_{\overline{NO3}} \cdot g_x^{-1}$]
z	culture depth in the PBR[m]

Abbreviations

BBM	Bold's Basal Medium
Chl-a	chlorophyll *a*
Chl-b	chlorophyll *b*
DMSO	dimethyl sulfoxide
DW	dry weight
HPLC	high performance liquid chromatography
LED	light emitting diode
LRPA	local rate of photon absorption
MRPA	mean rate of photon absorption
OD	optical density
PAR	photosynthetically active region
PBR	photobioreactor
PBS	phosphate buffer saline
PMMA	polymethyl methacrylate
TAG	triacylglycerol

Greek letters

λ	light wavelength[nm]
ρ_λ	diffuse reflectance of the PBR back wall[dimensionless]

astaxanthin accumulation mainly occurs in the red aplanospore morphotype, obtained under stressful conditions to trigger astaxanthin accumulation: excess light, salt or nitrogen deficiency [14,15]. Under these conditions, *H. pluvialis* synthesizes astaxanthin and stores it in fat globules [16,17].

Currently, the industrial production of astaxanthin by *H. pluvialis* follows a two-stage batch mode, first producing biomass under optimal growth conditions and then exposing cells to stressful conditions to induce the carotenogenesis [12,15,18–26]. The separation of biomass production and astaxanthin accumulation stages leads to rather large cultivation surfaces, as at least two culture systems are required, increasing then the production cost of astaxanthin [27,28]. This was also mentioned that red aplanospores provide poor astaxanthin bioavailability when ingested directly, due to the presence of a thick sporopollenin cell wall [29,30]. Disruption of these cell walls has also proven difficult even when using harsh treatments including acetolysis and autoclaving, also invariably resulting in losses of astaxanthin [31,32].

Continuous one-stage approach for producing an astaxanthin-enriched biomass from *H. pluvialis* could reveal here of interest. It would simplify the industrial process, while enabling a better tuning of exploitation conditions, because of the possibility to achieve a steady-state and then stable physiological state and biochemical composition. The general approach is to conduct continuous culture under nitrogen-limited stress, enabling both biomass and astaxanthin simultaneous production in one culture system. This was already developed and tested in indoor and outdoor tubular PBRs and raceway ponds [28,33–35]. A low astaxanthin content was obtained (about 1.1 % DW) with a low astaxanthin purity (65 % of total carotenoids) [28,33,34] when compared with current two-stage system modes [12,21,26,36,37]. However, interestingly, >90 % of the cells were found of reddish vegetative type, either flagellated or palmelloïd, with the presence of only a small fraction of hard-walled aplanospores. Reddish vegetative cells generated under continuous culture were indeed found lacking of hard cell wall, facilitating then carotenoid extraction through cell disruption with mild treatments, therefore reducing the extraction cost and increasing bioavailability of astaxanthin [28]. Moreover, this reddish biomass was also found rich in both astaxanthin and fatty acids, exhibiting then high antioxidant activity, analogous to that of red aplanospore cysts [38].

Similarly with astaxanthin production from *H. pluvialis*, nitrogen deprivation is known to trigger lipids accumulation in microalgae. It was then widely studied, especially in the perspective of microalgae-based biofuel production for producing microalgal biomass enriched in lipids. We demonstrated a strong relation with the light received per cell, either in batch [39,40] or continuous mode [41,42]. In continuous mode, a tight optimization of both the nitrogen concentration in the feeding medium and the incident photon flux density (PFDs) revealed to significantly increase lipids (i.e. triacylglycerol) accumulation and productivity. This was explained by the direct relation of lipid metabolism to photosynthetic process: nitrogen deprivation but also photon absorption rate by the culture were found of primary relevance. Recently, Heredia et al. [42] investigated the efficiency of TAG production by *Nannochloropsis gaditana* in both batch and continuous cultures, and concluded that the TAG productivity was higher under continuous nitrogen limitation but with appropriate photon absorption rate.

Samhat et al. [43] demonstrated recently a correlation between the astaxanthin accumulation and productivity by *H. pluvialis*, and the mean rate of photon absorption (MRPA) defined as a function of incident irradiance and light attenuation in the PBR. Experiments were conducted in batch conditions. Under these conditions, the optimization of the MRPA in the PBR was found to be difficult due to the complex influence of both biomass concentration and cells pigmentation (including astaxanthin accumulation) on the light attenuation conditions in the PBR, and the continuous time evolution of these parameters. Therefore, continuous cultures where all physiological parameters of the culture can achieve a steady-state appears here of interest for studying astaxanthin metabolism with regard to the light absorption by cells, and for optimizing these culture conditions to improve astaxanthin productivity by *H. pluvialis*.

This study aims therefore to develop an optimized protocol for continuously producing an astaxanthin-enriched biomass issued from *H. pluvialis* grown in nitrogen-limited conditions in artificial-light PBR. Given that astaxanthin accumulation is influenced by photosynthesis, we have developed in our study a methodology similar to the one

previously employed to enhance the continuous production of lipid-rich biomass [41,42]. Different incident photon flux densities (PFD) and nitrogen concentration in the feeding medium were applied in continuous culture (i.e. chemostat mode). Results were then analyzed in terms of growth kinetics and astaxanthin accumulation, but also of light transfer conditions as represented by the mean rate of photon absorption (MRPA). Kandilian et al. [40,41] showed indeed that the MRPA, when combined with a nitrogen limitation conditions, controls the accumulation of reserves as triacylglycerol by *Nannochloropsis oculata* and *Parachlorella kessleri*. It was then expected a similar result here on astaxanthin from *H. pluvialis*, so as to demonstrate the interest of the MRPA to find the good balance in culture conditions to maintain growth under nitrogen-limited conditions, while triggering significant astaxanthin accumulation in reddish vegetative cells.

2. Light transfer modeling

Because of the light attenuation that occurs in the culture volume, numerous kinetic models have been developed for coupling microalgae biomass and/or metabolite productivity to light transfer in the culture volume [44–49]. The specific local rate of photon absorption (LRPA), noted $\mathscr{A}$ [50], revealed of interest when coupling light-related kinetics (i.e. photosynthesis) to light transfer conditions. $\mathscr{A}$ represents the amount of photon absorbed in the spectral range of photosynthetic active radiation (PAR, between 400 and 700 nm) per unit weight of biomass and per unit time, and is expressed in $\mu mol_{h\nu}\ kg_x^{-1}{\cdot}s^{-1}$. $\mathscr{A}$ depends on the absorption cross-section $A_{abs,\lambda}$ of the microalgae (and then of cells pigmentation) and of the spectral fluence rate $G_\lambda(z)$ obtained at a given depth of culture. As a result, $\mathscr{A}_\lambda(z)$ is a local value $\left(\mathscr{A}_\lambda(z) = A_{abs,\lambda}G_\lambda(z)\right)$ which has to be averaged on both the PAR region and the total culture volume to obtain the mean rate of photon absorption (MRPA or $<\mathscr{A}>$).

For a flat-panel PBR, as used in this study, it is simply obtained by averaging local values $\mathscr{A}$ over the culture depth z [51]:

$$MRPA = <\mathscr{A}> = \frac{1}{L}\int_{400}^{700}\int_{0}^{L}\mathscr{A}_\lambda(z)dzd\lambda = \frac{1}{L}\int_{400}^{700}\int_{0}^{L}A_{abs,\lambda}G_\lambda(z)dzd\lambda \quad (1)$$

where $A_{abs,\lambda}$ is the spectral mass absorption cross-section of the microalgae (in $m^2{\cdot}kg^{-1}$), $G_\lambda(z)$ is the local fluence rate at depth z (in $\mu mol_{h\nu}{\cdot}m^{-2}{\cdot}s^{-1}$), L is the thickness of the PBR (in m) and λ is the light wavelength (in nm).

In the case of microalgal culture, the local spectral fluence rate $G_\lambda(z)$ can be obtained by solving the radiative transfer equation [52]. For geometries responding to the one-dimensional hypothesis, like in the case of flat-panel PBR, the two-flux model proved also effective to properly describe light diffusion and absorption phenomena in algal suspensions [53]. This requests however to determine the backward scattering ratio defined as the fraction of the radiation scattered backwards, which is estimated from the suspension's scattering phase function. It was measured for different species of microalgae [40,41] but for *H. pluvialis*, this value has not yet been measured. But because the backward scattering ratio is very low for microalgae cells, Lee et al. [54] and Kandilian et al. [55] demonstrated that a simplified method only based on absorption properties could be used to determine the fluence rate field and then MRPA with negligible error, leading to:

$$G_\lambda(z) = q_{\lambda,0}exp\left(-A_{abs,\lambda}C_x z\right) + \rho_\lambda q_{\lambda,0}exp\left(-A_{abs,\lambda}C_x(2L-z)\right) \quad (2)$$

where $q_{\lambda,0}$ is the incident PFD (in $\mu mol_{h\nu}{\cdot}m^{-2}{\cdot}s^{-1}$) and ρ_λ represents the diffuse reflectance of the PBR back wall ($\rho_\lambda = 0$ for transparent back wall).

Following Eq. (2), the simplified expression for the fluence rate $G_\lambda(z)$ depends only on the spectral mass absorption cross-section $A_{abs,\lambda}$ of the microalgal suspension, which has to be accurately determined using a spectrophotometer with an integrating sphere to take into account from the light scattering by microalgae cells [55]. This method was recently used and validated by Ferrel Ballestas et al. [56] for a culture of *Chlamydomonas reinhardtii* cultivated in PBRs under progressive nitrogen starvation conditions.

The PAR-averaged fluence rate $G(z)$ can be then obtained by integrating the local values $G_\lambda(z)$ over the PAR region as:

$$G(z) = \int_{400}^{700}G_\lambda(z)d\lambda \quad (3)$$

3. Materials and methods

3.1. Strain and culture medium

The algal strain *Haematococcus pluvialis* SAG 34–7 was obtained from the Culture Collection of Algae at the University of Göttingen, Germany. It was cultivated in modified Bold's Basal Medium (BBM; [57]) with the following composition (in mM): $NaNO_3$ 8.824, $MgSO_4{\cdot}7H_2O$ 0.913, $CaCl_2{\cdot}2H_2O$ 0.17, $Na_2EDTA{\cdot}2H_2O$ 0.134, $FeSO_4{\cdot}7H_2O$ 0.05, K_2HPO_4 0.861, KH_2PO_4 0.9, $ZnSO_4{\cdot}7H_2O$ 7.72×10^{-4}, $Co(NO_3)_2{\cdot}6H_2O$ 1.51×10^{-4}, $CuSO_4$ 6.25×10^{-7}, H_3BO_3 4.6×10^{-5}, $MnCl_2{\cdot}4H_2O$ 9.15×10^{-6}, Na_2MoO_4 1.063×10^{-3} and $NaHCO_3$ 15.

The culture strategy followed in this study was to feed the culture with a BBM culture medium containing all the nutrients in sufficient quantities, except for sodium nitrate ($NaNO_3$), the concentration of which was lower than that necessary to ensure optimal growth. It was therefore a nitrogen limitation in continuous mode, where the low concentrations of $NaNO_3$ used (3 and 1 mM) can make it possible to trigger an accumulation of astaxanthin while maintaining good growth of the microalgae.

3.2. Cultivation method

H. pluvialis was cultivated in a 1 L airlift-type flat panel PBR with a thickness L of 3 cm and a specific illuminated surface a_{light} of 33.33 m^{-1}. The PBR was described in more detail in Pruvost et al. [58]. The PBR was continuously illuminated on one side by a white LED light panel with adjustable PFD. The illuminated surface of the PBR was made of transparent polymethyl methacrylate (PMMA) and the backwall of diffuse stainless steel.

The PBR was set with a complete loop of common sensors and automation for microalga culture, namely pH, temperature, and gas injections (CO_2 and air). The pH was measured using a pH sensor (InPro48XX, Mettler-Toledo AG, Greifensee, Switzerland) and was set to 7.5 ± 0.2 by the injection of CO_2 inside the PBR when the measured pH exceeded the set point, and the temperature was kept stable at room temperature in a temperature-controlled room set at 22 ± 2 °C. The incident PFD was measured over the PAR region at nine different locations on the inside surface of the PBR using a quantum light sensor (Li-250A, Li-COR, Lincoln, NE). Before starting each experiment, the PBR was sterilized for 30 min using a 5 mM peroxyacetic acid solution and rinsed twice with sterile deionized water.

Initially, the PBR was inoculated with batch-grown cells for about 4–5 days at low PFD (50 $\mu mol_{h\nu}{\cdot}m^{-2}{\cdot}s^{-1}$) until reaching a sufficient biomass concentration to switch to continuous mode. Then, the culture was changed to continuous chemostat mode, fresh medium being continuously fed to the PBR, using a peristaltic pump (Ismatec, Reglo Digital MS-2/6, ISM 831-C, Wertheim, Germany), at a constant dilution rate. The culture was harvested by overflowing the PBR into a sterile harvest bottle.

In this study, the PBR was exposed to several incident PFDs (75–150–250–500 and 750 $\mu mol_{h\nu}{\cdot}m^{-2}{\cdot}s^{-1}$) with a continuous medium feed, at a constant dilution rate D of 0.015 h^{-1}, containing different nitrate concentration levels [NO_3^-] (1, 3 and 8.8 mM which correspond to 62, 186 and 547 $mg{\cdot}L^{-1}$ respectively) while keeping the other

components of the medium constant.

First, a continuous culture of *H. pluvialis* under normal growth conditions was carried out as a reference. The [NO_3^-] in the culture medium was 8.8 mM (i.e. without limitation) and the incident PFD was 75 $\mu mol_{h\nu} \cdot m^{-2} \cdot s^{-1}$. Once steady state was reached and the culture became stable, the experiments were conducted under nitrogen-limiting conditions to trigger carotenoids accumulation while maintaining cells growth. For each of these conditions, the biomass, chlorophyll (a and b) and astaxanthin content were determined at steady state. The residual nitrogen concentration in the culture was measured by ion chromatography (see next).

3.3. Analytical methods

3.3.1. Dry weight and biomass productivity

Microalgae dry weight concentration C_x was measured gravimetrically by filtering given culture volume through a pre-dried and pre-weighed glass-fiber filter (Whatman GF/F, 0.47 μm pore size, VWR, France). The filters were dried at 105 °C for at least 24 h and then reweighed after being cooled in a desiccator for 10–15 min. The samples were analyzed in triplicates and the reported biomass concentration corresponded to the mean value.

The volumetric biomass productivity P_x (in $g \cdot m^{-3} \cdot d^{-1}$) in the continuous cultures at dilution rate D (in d^{-1}) was calculated from biomass concentration C_x (in $g \cdot m^{-3}$) measured at steady state 3 days in a row [59]. Measurements of productivities were taken in triplicate on three consecutive days.

$$P_x = C_x D \tag{4}$$

$$Y_{NO_3^-/x} = \frac{[NO_3^-] - [NO_3^-]_r}{C_x} \tag{6}$$

where [NO_3^-] is the nitrate concentration in the feeding medium (in $mg \cdot L^{-1}$ or $g \cdot m^{-3}$) and $[NO_3^-]_r$ is the residual nitrate concentration in the culture (in $mg \cdot L^{-1}$ or $g \cdot m^{-3}$). Note that nitrogen limitation occurs for very low nitrate concentration in the culture medium [41,42,60]. So, in most cases $[NO_3^-]_r \approx 0$.

The nitrate availability was then quantified as the Specific Nitrate Input SNI, according to Del Río et al. [33]. The term SNI refers to the amount of nitrate (in mg NO_3^-) made available to cells (in g of DW) per time unit (in day). The SNI (in $mg_{NO3}^- \cdot g_x^{-1} \cdot d^{-1}$) was calculated as follow:

$$SNI = Y_{NO_3^-/x}\, D \tag{7}$$

3.3.4. Pigment concentration

Pigments were extracted and quantified spectrophotometrically. According to Qiu et al. [61], a volume V_1 (in mL) of *H. pluvialis* culture was first centrifuged at 13400 rpm for 15 min. The medium was discarded and the cells were resuspended in a volume V (in mL) of dimethyl sulfoxide (DMSO) and then incubated at 50 °C for 1–2 h in the dark until the sample turned white. After cooling, the pigment extract was diluted with a volume V_2 (in mL) of 90 % acetone (the ratio of DMSO: 90 % acetone should be equal to 1:4) and was then centrifuged at 13400 rpm for 15 min. The optical density OD_λ of the supernatant was measured at 630, 645, 665 and 750 nm with a UV–vis spectrophotometer (JASCO V-630). All extractions were performed in triplicates. Chlorophyll a (Chl-a) and b (Chl-b) concentrations (in $g \cdot m^{-3}$) were calculated as follow [62]:

$$\begin{aligned} C_{chl-a} &= [11.6\,(OD_{665} - OD_{750}) - 1.31\,(OD_{645} - OD_{750}) - 0.14\,(OD_{630} - OD_{750})]\,\frac{V_2}{V_1 l} \\ C_{chl-b} &= [20.7\,(OD_{645} - OD_{750}) - 4.34\,(OD_{665} - OD_{750}) - 4.42\,(OD_{630} - OD_{750})]\,\frac{V_2}{V_1 l} \end{aligned} \tag{8}$$

The areal biomass productivity S_x ($g \cdot m^{-2} \cdot d^{-1}$) was then deduced from the specific illuminated surface a_{light} (in m^{-1}) of the PBR, defined by the ratio of illuminated surface S_{light} and volume V_r of culture, as follow:

$$S_x = P_x \frac{V_r}{S_{light}} = \frac{P_x}{a_{light}} \tag{5}$$

3.3.2. Microscopic observation

The morphological changes in cells were observed using an optical microscope (Zeiss, Axio, Imager.M2m, Jena, Germany) connected to a CCD camera (Zeiss, AxioCam MRc, Jena, Germany), in order to follow the progress of the cell morphology of *H. pluvialis* under stressed conditions.

3.3.3. Nitrate availability and yield

Once a steady state was reached in the continuous cultures, a volume of 3–5 mL of culture was filtered using a 0.2 μm acetate cellulose filter (Minisart, Sartorius, Göttingen, Germany). The filtrate was injected into an ion chromatography system (ICS 900, Thermo Fisher Sci, Waltham, Massachusetts, USA) to measure the residual nitrate concentration in the culture $[NO_3^-]_r$. If needed, concentration was adjusted by dilution with ultra-pure water (Milli-Q) to make concentrations in the range of linearity of the calibration curve.

The Nitrate uptake Yield $Y_{NO_3^-/x}$ (in $mg_{NO3}^- \cdot g_x^{-1}$) was then calculated as:

where V_1 is the culture sample volume (in mL), V_2 is the volume of added acetone (in mL) and l is the cuvette path length (1 cm).

The corresponding mass fraction of pigment 'i' per dry weight of biomass W_i (in DW %) can be estimated as:

$$W_i = \frac{C_i}{C_x}\, 100 \tag{9}$$

where C_i is the pigment concentration (in $g \cdot m^{-3}$).

3.3.5. Astaxanthin content determination

3.3.5.1. Spectrophotometric measurement. Astaxanthin was extracted in DMSO and quantified spectrophotometrically according to the method published by Boussiba et al. [63]. The harvested algae cells V_1 were collected by centrifuging at 11000 rpm for 10 min, first treated to destroy the chlorophyll with a solution of 5 % (*w/v*) KOH in 30 % (*w/w*) methanol at 70 °C for 10 min. The supernatant was discarded, and the remaining pellet was extracted with a volume V_2 of DMSO after adding 100 μL of acetic acid and applying homogenization (by vortex) for astaxanthin recovery (acetic acid should be added before the addition of the DMSO otherwise the pellet will agglomerate and it will be difficult to perform the extraction). The extract was then heated for 30 min at 70 °C. The red supernatant was collected (after centrifugation for 10 min at 11000 rpm), the optical density at 490 nm was measured and the astaxanthin concentration C_{asta} (in $g \cdot m^{-3}$) was calculated according to the following equation [37]:

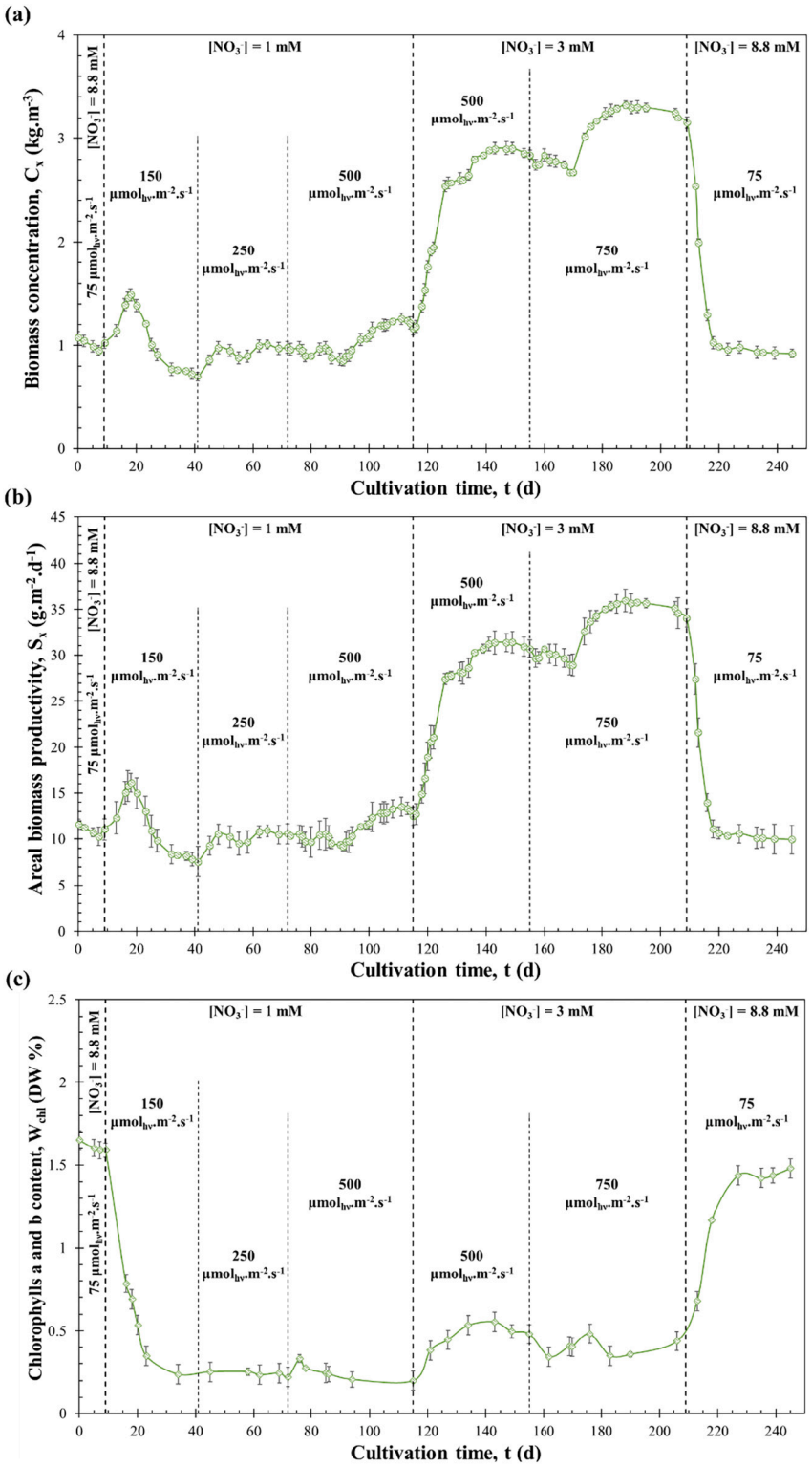

Fig. 1. (a) Biomass concentration C_x, (b) areal biomass productivity S_x and (c) chlorophyll content W_{chl} of *H. pluvialis* culture grown in chemostat mode with a constant dilution rate D of 0.015 h^{-1} under different incident photon flux densities PFDs and nitrate concentration [NO_3^-] levels in the feeding medium as a function of cultivation time t. Data are shown as mean ± SD, $n = 3$.

$$C_{asta} = 4.5\ OD_{490}\ V_1\ V_2 \quad (10)$$

where V_1 is the culture sample volume (in mL), V_2 is the volume of added DMSO (in mL) and OD_{490} is the extract optical density at 490 nm.

The astaxanthin content W_{asta} (in DW %) was then calculated:

$$W_{asta} = \frac{C_{asta}}{C_x} 100 \quad (11)$$

The volumetric astaxanthin productivity P_{asta} (in $g{\cdot}m^{-3}{\cdot}d^{-1}$) was then calculated:

$$P_{asta} = C_{asta}\ D \quad (12)$$

The areal astaxanthin productivity S_{asta} (in $g{\cdot}m^{-2}{\cdot}d^{-1}$), for a flat-panel PBR, was then calculated as:

$$S_{asta} = \frac{P_{asta}}{a_{light}} = P_{asta}\ L \quad (13)$$

3.3.5.2. HPLC analysis. In order to identify the different carotenoids present in the *H. pluvialis* cells at the steady state of each nitrogen-limited culture, single carotenoids (astaxanthin, β-carotene, lutein and zeaxanthin) were quantified, according to Su et al. [64]. This analysis was performed using high-performance liquid chromatography (HPLC) equipped with a Diode Array Detector (HPLC-DAD) (Agilent 1260 Infinity II, Santa Clara, CA). Detection wavelengths for integration ranged from 190 to 800 nm, with chromatographic peaks measured at 480 nm to facilitate the detection of astaxanthin. A LiChroCART® RP C18 column (5 µm, 250 × 4.6 mm, LiChrosorb, Merck KGaA, Germany) was used for reverse-phase chromatography during a 80 min elution program at 30 °C. The mobile phases consisted of solvent A (water/methanol: 1/4 v/v), and solvent B (acetone/methanol: 1/1 v/v). The flow rate was 0.5 $mL{\cdot}min^{-1}$ and the sample injected volume was 40 µl.

The purity of astaxanthin was then quantified as the fraction of astaxanthin relative to total carotenoids f_{asta} (in total carotenoids %) as follow:

$$f_{asta} = \frac{C_{asta}}{C_{total-coratenoids}} 100 \quad (14)$$

where C_{asta} is the astaxanthin concentration (in $g{\cdot}m^{-3}$) and $C_{total\text{-}carotenoids}$ is the total carotenoids concentration (in $g{\cdot}m^{-3}$), measured by HPLC at the steady state of each culture condition.

3.3.6. Experimental measurements of radiation characteristics

The radiation characteristics (i.e. the mass absorption cross-sections $A_{abs,\lambda}$) of the microorganisms were measured using the method described by Kandilian et al. [55]. The normal-hemispherical transmittance $T_{nh,\lambda}$ and reflectance $R_{nh,\lambda}$ of *H. pluvialis* suspensions, with biomass concentration ranging from 0.1 to 10 $kg{\cdot}m^{-3}$, were measured using the internal integrating sphere accessory (Agilent Cary DRA-2500, Santa Clara, CA) of the UV–Vis-NIR spectrophotometer (Agilent Cary 5000, Santa Clara, CA).

The microalgal samples were centrifuged at 11000 rpm for 15 min at 15 °C and washed twice with phosphate buffer saline (PBS) solution before measurements, in order to avoid absorption and scattering by the growth medium, and then suspended in PBS. The volume of culture sampled and PBS used were chosen based on the biomass concentration desired for optical measurements (0.1 to 10 $kg{\cdot}m^{-3}$). Quartz cuvettes of 1 cm depth were used (110-10-40 Hellma Analytics, Müllheim, Germany). The $T_{nh,\lambda}$ and $R_{nh,\lambda}$ experimentally measured in the wavelength range from 350 to 750 nm (1 nm spectral resolution) were then used as input parameters in an inverse method to retrieve the spectral mass absorption cross-sections $A_{abs,\lambda}$ of *H. pluvialis*. The $A_{abs,\lambda}$ was then used to calculate the MRPA and $G_\lambda(z)$ for each culture condition.

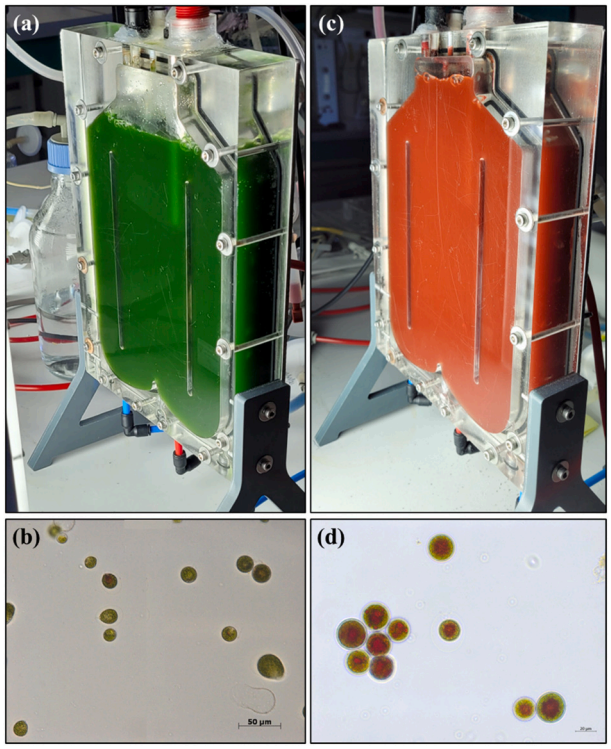

Fig. 2. Airlift PBR and microscopic view of *H. pluvialis* cultures in: (a,b) green phase and (c,d) red phase. Scale bars: (b) 50 µm and (d) 20 µm. (For interpretation of the references to color in this figure legend, the reader is referred to the web version of this article.)

4. Results and discussion

4.1. Biomass and chlorophyll concentrations

Fig. 1 shows the time evolution of biomass concentration C_x and productivity S_x, and chlorophyll *a* and b content W_{chl} of *H. pluvialis* grown in a PBR operated in chemostat mode with a constant dilution rate of 0.015 h^{-1}. Different incident PFDs of 75, 150, 250, 500 and 750 $\mu mol_{h\nu}{\cdot}m^{-2}{\cdot}s^{-1}$ and $[NO_3^-]$ levels in the feeding medium of 8.8, 3 and 1 mM were used to trigger astaxanthin accumulation.

Under low light intensity and nitrogen sufficiency (i.e. PFD = 75 $\mu mol_{h\nu}{\cdot}m^{-2}{\cdot}s^{-1}$ and $[NO_3^-]$ = 8.8 mM), the steady state C_x and S_x values were respectively 1.02 $kg{\cdot}m^{-3}$ and 11.02 $g{\cdot}m^{-2}{\cdot}d^{-1}$. Under these conditions, the culture exhibited green color (c.a. 1.59 % DW chlorophyll and only 0.24 % DW astaxanthin), the cell population being mostly composed of green vegetative motile cells (Fig. 2a and b) with a proportion of palmelloïd cells under 20 % (data not shown).

After reducing the $[NO_3^-]$ in the feeding medium from 8.8 mM to 1 mM and increasing the incident PFD from 75 to 150 $\mu mol_{h\nu}{\cdot}m^{-2}{\cdot}s^{-1}$, there was an initial increase in biomass concentration up to 1.49 $kg{\cdot}m^{-3}$. As also observed by Kandilian et al. [41] and Heredia et al. [42], this was attributed to a transient increase in the rate of photon absorption in the PBR due to the deeper penetration of light in the PBR culture as a consequence of the significant decrease in chlorophyll content of the cells, as shown in Fig. 1. However, once the culture reached the new steady state conditions, C_x, S_x and W_{chl} values were equal to 0.77 $kg{\cdot}m^{-3}$, 8.32 $g{\cdot}m^{-2}{\cdot}d^{-1}$ and 0.43 % DW, respectively.

After increasing the incident PFD from 150 to 500 $\mu mol_{h\nu}{\cdot}m^{-2}{\cdot}s^{-1}$, C_x and S_x values increased and reached 1.21 $kg{\cdot}m^{-3}$, 13.07 $g{\cdot}m^{-2}{\cdot}d^{-1}$ respectively, while the W_{chl} value decreased and was equal to 0.21 % DW at the new steady state. Then, the increase in $[NO_3^-]$ in the feeding medium, from 1 to 3 mM, resulted in moderate nitrogen limitation, and an increase in biomass concentration and productivity and chlorophyll

content was observed. The steady state C_x, S_x and W_{chl} values were respectively, 2.89 kg·m^{-3}, 31.21 g·m^{-2}·d^{-1} and 0.48 % DW, when the incident PFD and the [NO_3^-] in the feeding medium were 500 $\mu mol_{h\nu}\cdot m^{-2}\cdot s^{-1}$ and 3 mM, respectively.

After increasing the incident PFD from 500 to 750 $\mu mol_{h\nu}\cdot m^{-2}\cdot s^{-1}$, C_x and S_x values increased and reached 3.22 kg·m^{-3}, 34.78 g·m^{-2}·d^{-1} respectively, while the W_{chl} value slightly decreased and was equal to 0.44 % DW at the new steady state. Under these conditions of low nitrate availability (20.8 $mg_{NO3}\cdot g_x^{-1}\cdot d^{-1}$) and high PFDs, the cultures turned red (chlorophyll content W_{chl} did not exceed 0.25 % DW), with reddish palmelloïd cells (Fig. 2c and d) becoming the most abundant cell morphotype, higher than 80 % (data not shown).

As expected, in nitrogen-limited conditions, the culture with the smallest [NO_3^-] (i.e. 1 mM) and incident PFD (i.e. 150 $\mu mol_{h\nu}\cdot m^{-2}\cdot s^{-1}$) featured the smallest biomass and chlorophyll concentrations, while the highest biomass concentration of 3.22 kg·m^{-3}, corresponding to 34.78 g·m^{-2}·d^{-1}, was achieved when [NO_3^-] was 3 mM and at the highest incident PFD of 750 $\mu mol_{h\nu}\cdot m^{-2}\cdot s^{-1}$, illustrating that biomass and chlorophyll concentrations changed in a disproportionate amounts and in an apparent unpredictable way in response to nitrogen limitation (MRPA analysis will give better insight in those results).

The last step of the experiment was to test the reversibility of the process by returning the culture to initial normal growth conditions (i.e. PFD = 75 $\mu mol_{h\nu}\cdot m^{-2}\cdot s^{-1}$ and [NO_3^-] = 8.8 mM) in order to reach again the green phase. As expected, red cells then return into green phase, and rebuild their chlorophyll content. The steady state biomass concentration C_x and productivity S_x and chlorophyll content W_{chl} of the culture were 0.94 kg·m^{-3}, 10.15 g·m^{-2}·d^{-1} and 1.48 % DW, respectively, that was approximately the same values at the start of the culture (before limitation), as shown in Fig. 1, where the cell population being mostly composed of green vegetative cells (higher than 80 % (data not shown)) (Fig. 2a and b).

4.2. Astaxanthin concentration and productivity

Fig. 3 plots the astaxanthin concentration C_{asta} and content W_{asta} of *H. pluvialis* as a function of cultivation time *t*. When the culture was grown in non-limited conditions, C_{asta} and W_{asta} values were respectively equal to 2.43 g·m^{-3} and 0.24 % DW (with 2.64 % of total carotenoids). Nitrogen-limited cultures featured a larger cellular astaxanthin content compared to those grown in the non-limited conditions.

Table 1 presents biomass and astaxanthin concentrations and productivities, chlorophyll content, nitrate uptake yield and specific nitrate input at the steady state of each culture condition applied (for

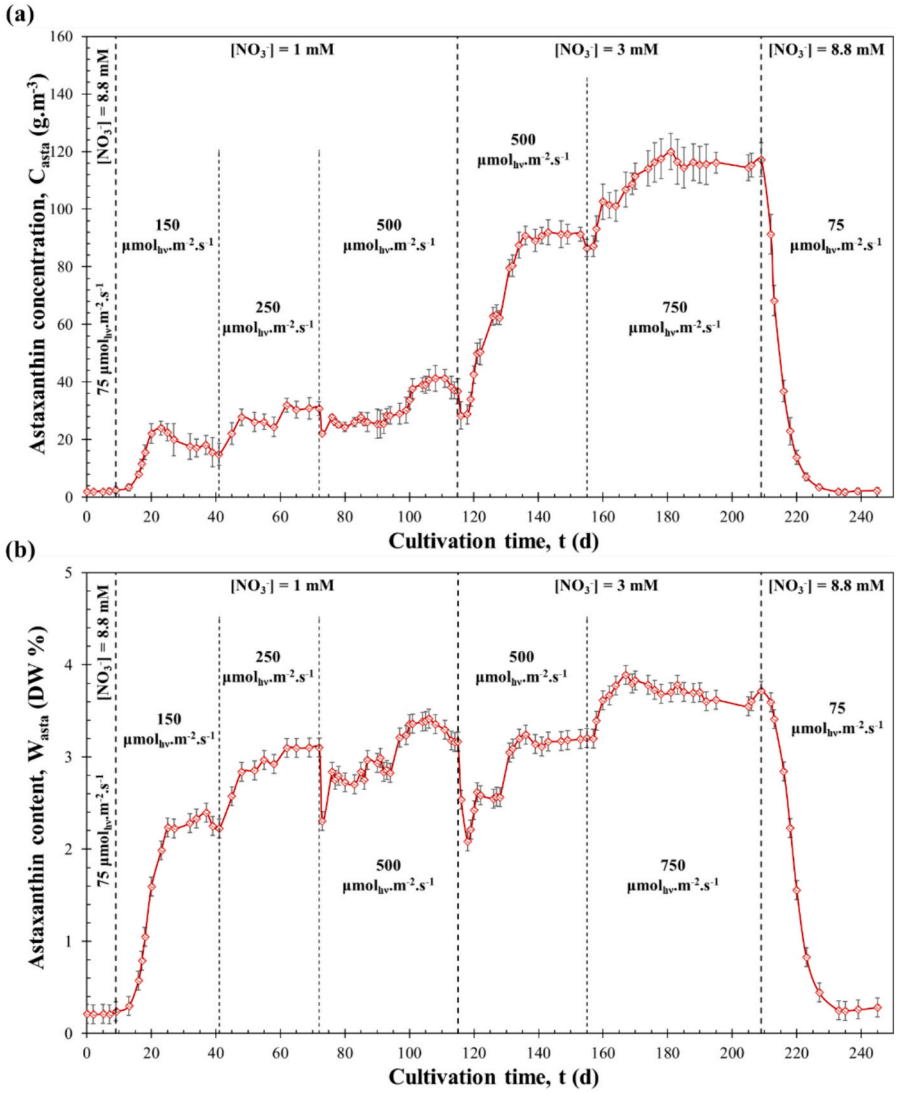

Fig. 3. Astaxanthin (a) concentration C_{asta} and (b) content W_{asta} of *H. pluvialis* culture grown in chemostat mode with a constant dilution rate *D* of 0.015 h^{-1} under different incident photon flux densities PFDs and nitrate concentration [NO_3^-] levels in the feeding medium as a function of cultivation time *t*. Data are shown as mean ± SD, $n = 3$.

Table 1
Steady state biomass and astaxanthin concentrations and productivities, chlorophyll content, nitrate uptake yield, specific nitrate input and mean rate of photon absorption for all culture conditions.

$[NO_3^-]$ (mM)	8.8	1	1	1	3	3	8.8
PFD ($\mu mol_{h\nu} \cdot m^{-2} \cdot s^{-1}$)	75	150	250	500	500	750	75
C_x ($kg \cdot m^{-3}$)	1.02	0.77	0.99	1.22	2.89	3.22	0.94
S_x ($g \cdot m^{-2} \cdot d^{-1}$)	11.02	8.32	10.69	13.18	31.21	34.78	10.15
W_{chl} (DW %)	1.59	0.23	0.23	0.21	0.48	0.45	1.48
C_{asta} ($g \cdot m^{-3}$)	2.43	17.21	30.96	37.74	92.61	125.31	2.21
W_{asta} (DW %)	0.24	2.24	3.13	3.12	3.20	3.89	0.24
S_{asta} ($g \cdot m^{-2} \cdot d^{-1}$)	0.03	0.19	0.33	0.41	0.99	1.27	0.02
f_{asta} (total carotenoids %)	2.64	96.78	97.52	98.22	98.05	98.36	2.27
$Y_{NO_3^-/x}$ ($mg_{NO3}^{-} \cdot g_x^{-1}$)	190.7	80.5	62.6	51.2	64.4	57.8	196.1
SNI ($mg_{NO3}^{-} \cdot g_x^{-1} \cdot d^{-1}$)	68.7	29	22.6	18.5	23.2	20.8	70.6
MRPA ($\mu mol_{h\nu} \cdot kg_x^{-1} \cdot s^{-1}$)	2586	4850	6099	11,440	6173	8915	2445

convenience, MRPA values were added, but they will be discussed later).

Maximum values of C_{asta} and W_{asta}, equal to 125.31 ± 5.35 $g \cdot m^{-3}$ and 3.9 ± 0.2 % DW, respectively were obtained when $[NO_3^-]$ was 3 mM and at the highest incident PFD of 750 $\mu mol_{h\nu} \cdot m^{-2} \cdot s^{-1}$. Under these conditions, the culture achieved both large biomass productivity and large cellular astaxanthin content, thus the highest S_{asta} of 1.27 ± 0.03 $g \cdot m^{-2} \cdot d^{-1}$. It corresponded also to a high astaxanthin purity (98.36 % of total carotenoids).

Regarding the nitrate assimilation, the nitrate uptake yield ($Y_{NO_3^-/x}$) and the specific nitrate input (SNI), indicating the ability and the rate of the cell to assimilate the surrounding nitrogen sources, were calculated at steady state for each limitation level. Note that all the limited cultures left an undetectable amount of $[NO_3^-]_r$ in the medium (<5 $mg_{NO3}^{-} \cdot L^{-1}$, below the detection level of ion chromatography), except for nitrogen-repleted condition (i.e. PFD = 75 $\mu mol_{h\nu} \cdot m^{-2} \cdot s^{-1}$ and $[NO_3^-]$ = 8.8 mM), confirming a situation of nitrogen limitation expected to stress the cultures by limiting the nitrogen source, regardless the applied light intensity.

The non-limited culture was characterized for the highest $Y_{NO_3^-/x}$ and SNI values of 193.4 ± 3.8 $mg_{NO3}^{-} \cdot g_x^{-1}$ and 69.6 ± 1.4 $mg_{NO3}^{-} \cdot g_x^{-1} \cdot d^{-1}$ respectively, where negligible astaxanthin accumulation was observed (0.24 % DW astaxanthin). The $Y_{NO_3^-/x}$ and SNI values were decreased to 80.5 $mg_{NO3}^{-} \cdot g_x^{-1}$ and 29 $mg_{NO3}^{-} \cdot g_x^{-1} \cdot d^{-1}$ when $[NO_3^-]$ was 1 mM and at an incident PFD of 150 $\mu mol_{h\nu} \cdot m^{-2} \cdot s^{-1}$. Then, $Y_{NO_3^-/x}$ and SNI values were decreased again for the others nitrogen-limited conditions (Table 1). The accumulation of astaxanthin was maximal (1.27 ± 0.03 $g \cdot m^{-2} \cdot d^{-1}$) for a $Y_{NO_3^-/x}$ and SNI values of 57.8 $mg_{NO3}^{-} \cdot g_x^{-1}$ and 20.8 $mg_{NO3}^{-} \cdot g_x^{-1} \cdot d^{-1}$ (a decrease of 70 % compared to the non-limited condition). This also corresponds to the larger PFD value applied during our experiments (750 $\mu mol_{h\nu} \cdot m^{-2} \cdot s^{-1}$), leading to both the largest biomass productivity and cellular astaxanthin content, as previously mentioned.

As a result, a maximum astaxanthin accumulation corresponds to the condition of maximum biomass productivity and leads to the maximum astaxanthin productivity. We can conclude, then, that nitrate limitation is the main factor triggering the accumulation of astaxanthin in the continuous system. However, it is also not sufficient for producing cells rich in astaxanthin. This was illustrated more clearly with the culture fed with the lowest $[NO_3^-]$ of 1 mM and with PFDs of 150, 250 and 500 $\mu mol_{h\nu} \cdot m^{-2} \cdot s^{-1}$. Here, the cells were nitrate-limited as evident by the drastic reduction in chlorophyll content in the culture (0.22 ± 0.01 % DW) but they did not accumulate large amounts of astaxanthin (17.21, 30.96 and 38.74 $g \cdot m^{-3}$ respectively). As shown in next section, those conditions also correspond to a decrease in the photon absorption rate, as a result of the nitrogen limitation owing to the low chlorophyll contents (0.23 % DW chlorophyll) and biomass concentrations. This illustrates the essential role of photosynthetic pigments (i.e. chlorophyll) and light absorption in the maintaining of cells growth and cellular mechanism of accumulation of astaxanthin in *H. pluvialis* cells in continuous mode.

The strong relation between light and nitrogen availabilities is consistent with previous findings suggesting that the specific nitrate input and the average light intensity were decisive parameters in determining astaxanthin content of the biomass, as well as productivity of the system. Del Río et al. [28,33,34] and García-Malea et al. [35] reported in their works, using the one-stage strategy for the production of *H. pluvialis* astaxanthin under indoor and outdoor conditions in closed tubular PBR, that the growth rate of the continuous photoautotrophic cultures was a hyperbolic function of the average light intensity and a threshold value of 167.4 $mg_{NO3}^{-} \cdot g_x^{-1} \cdot d^{-1}$ of SNI was required to stimulate astaxanthin accumulation. Cells were green and astaxanthin was present only in small quantities when SNI was above 167.4 $mg_{NO3}^{-} \cdot g_x^{-1} \cdot d^{-1}$. While below this value, under conditions of moderate nitrogen limitation, astaxanthin accumulated to reach cellular levels of up to 1 ± 0.1 % DW with a low astaxanthin purity (65 % of total carotenoids). However, an increase in the accumulation of astaxanthin was observed by increasing the light intensity when the nitrogen supply was limiting, but never in nitrogen sufficiency. For indoor experiences, mean biomass and astaxanthin productivity values of 28.5 ± 4.5 and 0.312 ± 0.042 $g \cdot m^{-2} \cdot d^{-1}$ respectively were achieved for a SNI of about 49.6 $mg_{NO3}^{-} \cdot g_x^{-1} \cdot d^{-1}$ and an average light intensity range of 77–110 $\mu mol_{h\nu} \cdot m^{-2} \cdot s^{-1}$, while in outdoor experiments, biomass and astaxanthin productivity of 4.38 ± 0.63 and 0.05 ± 0.01 $g \cdot m^{-2} \cdot d^{-1}$, were obtained, respectively, for a SNI of about 31 $mg_{NO3}^{-} \cdot g_x^{-1} \cdot d^{-1}$.

It must be noted that values obtained in Del Río et al. [28,33,34] and García-Malea et al. [35] are much lower than those obtained in our study. To our knowledge, this is the highest reported astaxanthin content and productivity of *H. pluvialis* cells grown in nitrogen limitation continuous culture. Compared with two-stage production of astaxanthin [12,21,26,36,37,65], the advantage of the one-stage process is that it does not need to divide the production process into two parts with two bioreactors, therefore, the technique is simplified and a decrease in production cost is then expected. Another important advantage - other than the largest astaxanthin and biomass productivity - is the high astaxanthin purity obtained in our one-stage system which was higher than 95 % of total carotenoids for all nitrogen-limited cultures (Table 1).

Finally, in the last step of our experiment (i.e. PFD = 75 $\mu mol_{h\nu} \cdot m^{-2} \cdot s^{-1}$ and $[NO_3^-]$ = 8.8 mM), results show that, after the limitation, the same steady state reached at the start of the culture was obtained again, as shown in Figs. 1 and 3 and Table 1. These observations evidence the reversibility of the biological response. The one-stage culture allows then a high control of the physiological stage of *H. pluvialis*, enabling to increase both astaxanthin accumulation and productivity, making it an alternative of interest to replace the current widely employed two-stage approach.

4.3. Radiation characteristics of H. pluvialis

4.3.1. Mass absorption cross-section

Fig. 4 shows the spectral mass absorption cross-sections $A_{abs,\lambda}$ of *H. pluvialis* cells grown in chemostat mode with different culture

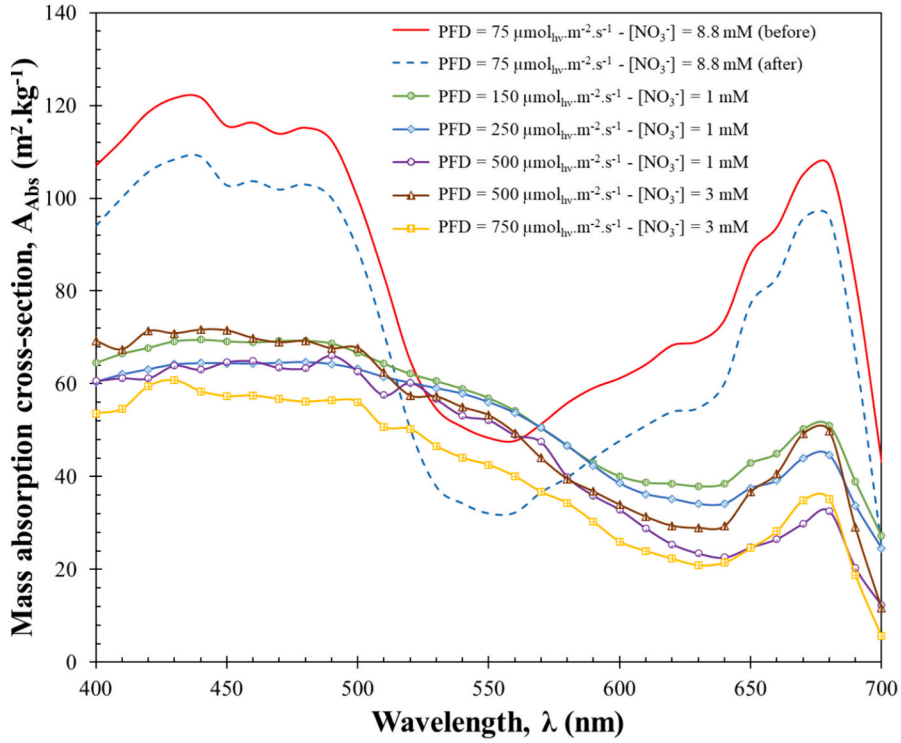

Fig. 4. The spectral mass absorption cross-section $A_{abs,\lambda}$ of *H. pluvialis* culture grown in chemostat mode with a constant dilution rate D of 0.015 h^{-1} under different incident photon flux densities PFDs and nitrate concentration [NO_3^-] levels in the feeding medium as a function of wavelength λ.

conditions applied. As previously observed for *Nannochloropsis oculata* and *Parachlorella kessleri* in Kandilian et al. [40,41], $A_{abs,\lambda}$ decreased across all wavelengths with decreasing nitrogen concentration in the medium. The overall decrease in $A_{abs,\lambda}$ was found mainly consistent with the reduction in cellular chlorophyll concentration, although changes in $A_{abs,\lambda}$ may also be attributed to any change in cell size or biochemical composition of the cells [52]. The magnitude and the shape of the $A_{abs,\lambda}$ of *H. pluvialis* cultures changed slightly for cultures grown with different [NO_3^-] and incident PFDs. For instance, the mass absorption cross-sections at 435 nm $A_{abs,435}$ and 676 nm $A_{abs,676}$, corresponding to chlorophyll *a* absorption peaks, decreased by 46 % and 63 % respectively when the [NO_3^-] in the feeding medium was adjusted from 8.8 mM to 3 mM and the incident PFD was increased from 75 to 750 µmol$_{hv}$·m^{-2}·s^{-1}, corresponding to the conditions of maximum production of astaxanthin, while the mass absorption cross-section at 550 nm $A_{abs,550}$, corresponding to the wavelength with lowest $A_{abs,\lambda}$, increased by 33 %. It can also be noted that rather similar $A_{abs,\lambda}$ were obtained before and after nitrogen-limited experiments, with a decrease of 16 % due to the slightly decrease in chlorophyll content at the end of culture (from 1.59 to 1.48 % DW). This confirmed the reversibility of the stressful conditions on *H. pluvialis* cultures.

4.3.2. Local fluence rate and rate of photon absorption

Using different [NO_3^-] levels in the feeding medium and different incident PFDs affect both biomass and chlorophyll concentrations in the culture, resulting in very different light attenuation conditions in the PBR culture volume. This was here analyzed through light transfer modeling.

Fig. 5a and b shows the PAR-averaged fluence rate $G(z)$ in the PBR and the corresponding specific local rate of photon absorption $\mathscr{A}$ respectively, for cultures with different [NO_3^-] levels and incident PFDs. Results confirm that the $G(z)$ and $\mathscr{A}$ changed in the PBR with absorption cross-section, biomass and pigment concentrations evolutions.

Cultures with higher fluence rate and rate of photon absorption at the back of the PBR ($G(L)$ and $\mathscr{A}(L)$ respectively) were found to feature lower biomass productivities (8.32, 10.69 and 13.18 g·m^{-2}·d^{-1}). Moreover, these cultures also suffered from relatively small MRPA (see Section 4.3.3) leading to the production of a relatively small cellular astaxanthin production (0.19, 0.33 and 0.41 g·m^{-2}·d^{-1}). Note that when cells are exposed to large $\mathscr{A}$, incident light to biomass or astaxanthin conversion may be locally inhibited due to the dissipation of energy by cells through fluorescence and heat [66]. In this case, the absorbed light can be wasted as heat rather than being directed into astaxanthin synthesis leading to a decrease in astaxanthin productivity. Such condition was encountered in the culture fed with the lowest [NO_3^-] of 1 mM and with an incident PFD of 500 µmol$_{hv}$·m^{-2}·s^{-1}. Increasing [NO_3^-] to 3 mM leads to higher content of both chlorophyll a and astaxanthin as well as higher productivities.

4.3.3. Mean rate of photon absorption

During nitrogen deprivation, *H. pluvialis* cells accumulate large amounts of photoprotective carotenoids (including astaxanthin), that absorb the incident radiant energy in order to quench it as heat and protect the photosystem [12,67]. Therefore, it is expected that some of the absorbed light energy will be released as heat and not be used for metabolism. Thus, determining the optimized value for light is not straightforward, as it involves increasing astaxanthin production while avoiding wasting too much light energy through photoprotective carotenoids.

Fig. 6a and b shows respectively the astaxanthin content W_{asta} (DW %) and the areal astaxanthin productivity S_{asta} (g·m^{-2}·d^{-1}) as a function of mean rate of photon absorption MRPA (µmol$_{hv}$·kg$_x^{-1}$·s^{-1}) in the PBR for the *H. pluvialis* cultures grown with different [NO_3^-] levels in the feeding medium and different incident PFDs. As a quantitative value of the light stress applied on the culture, the MRPA was calculated for the different conditions (Table 1). Interestingly, a clear correlation was found between the astaxanthin content and productivity, and the MRPA. In general, astaxanthin accumulation was found to increase monotonically with increasing MRPA. This observation is consistent with previous findings indicating that high light intensity and nitrogen

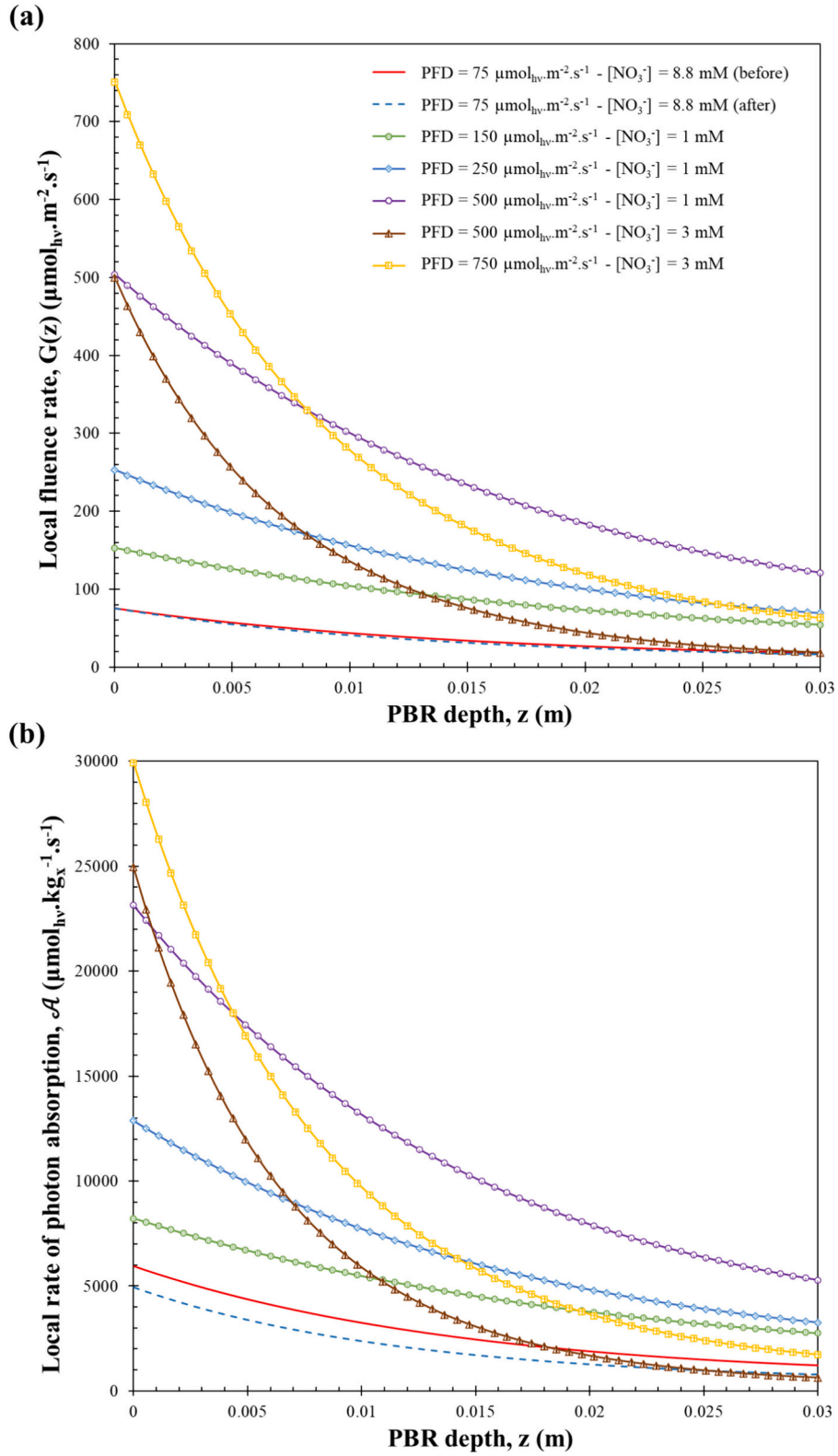

Fig. 5. (a) The PAR-averaged fluence rate $G(z)$ and (b) the specific local rate of photon absorption $\mathscr{A}$ of *H. pluvialis* culture grown in chemostat mode with a constant dilution rate D of 0.015 h^{-1} under different incident photon flux densities PFDs and nitrate concentration [NO_3^-] levels in the feeding medium as a function of PBR depth z.

starvation could improve astaxanthin production by dry weight [37]. However, the use of MRPA allows defining more accurately optimal conditions, as the MRPA depends not only on incident PFD, but also biomass concentration, cell pigment content and PBR characteristics (i. e. depth here).

This strong relation to MRPA is also consistent with the hypothesis that the astaxanthin's synthesis pathway is activated in order to quench excess electrons generated in the photosynthetic electron transport

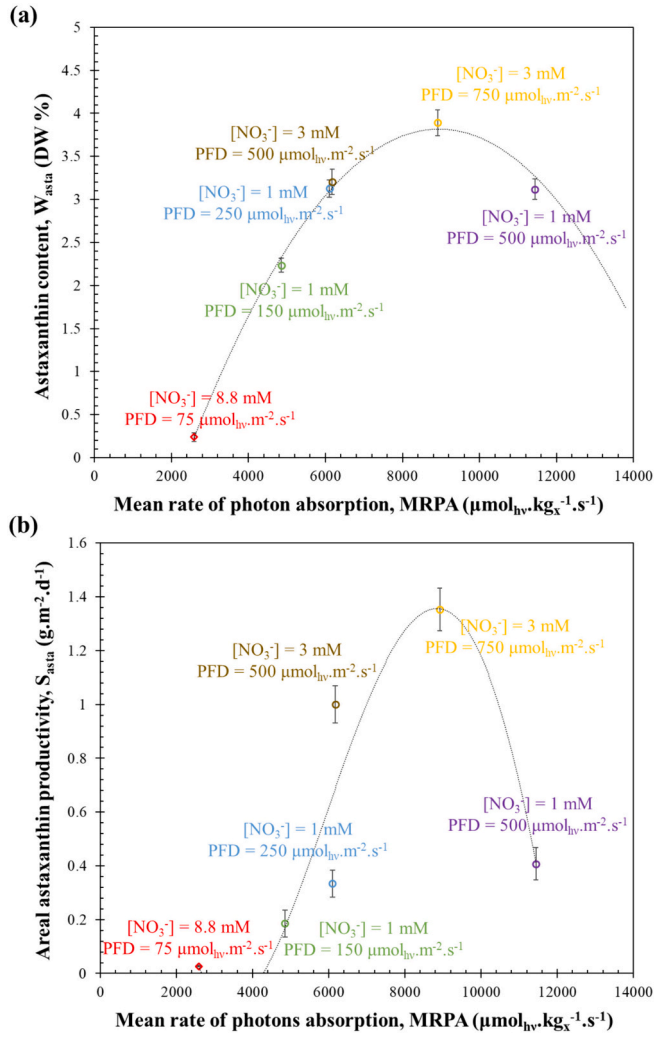

Fig. 6. (a) Cellular astaxanthin content W_{asta} and (b) areal astaxanthin productivity S_{asta} of *H. pluvialis* culture grown in chemostat mode with a constant dilution rate D of 0.015 h^{-1} under different incident photon flux densities PFDs and nitrate concentration [NO_3^-] levels in the feeding medium as a function of mean rate of photon absorption MRPA. Data are shown as mean ± SD, $n = 4$.

chain when cells receive a high light intensity and absorb large quantities of photon energy [12,67]. This excess energy is partly absorbed for the synthesis of astaxanthin to avoid cells damage by reactive oxygen species, since the synthesis of secondary carotenoids, compared to proteins and carbohydrates of similar mass, requires much more energy in the form of NADPH. Carotenoids such as β-carotene, lutein and astaxanthin are esterified along with TAG and stored in lipid bodies to protect cells from high light [12,67].

In regards to kinetics, similarly to results of Kandilian et al. [40,41] on lipids production, a parabolic relation between MRPA and astaxanthin content and productivity was obtained here. Note that the culture grown with a [NO_3^-] of 1 mM in the feeding medium and an incident PFD of 500 $\mu mol_{h\nu} \cdot m^{-2} \cdot s^{-1}$ featured the largest MRPA (11,440 $\mu mol_{h\nu} \cdot kg_x^{-1} \cdot s^{-1}$) but neither accumulate the largest W_{asta} (3.12 % DW) nor presented the largest S_{asta} (0.41 $g \cdot m^{-2} \cdot d^{-1}$). While, maximum astaxanthin content and productivity of 3.9 ± 0.2 % DW and 1.27 ± 0.03 $g \cdot m^{-2} \cdot d^{-1}$ respectively were reached for the culture featuring MRPA equal to 8915 $\mu mol_{h\nu} \cdot kg_x^{-1} \cdot s^{-1}$.

As recently discussed in our previous work [43], this complex relationship with MRPA indicates that nitrogen deprivation alone does not guarantee large astaxanthin production rate. The astaxanthin biosynthesis kinetics is here shown to be also related to both the photon absorption rate represented by MRPA and the photosynthetic capacity of the cells (i.e. chlorophyll content). So, increasing the MRPA beyond its optimal value results in a decrease in the astaxanthin productivity. However, due to the reduction in chlorophyll content and mass absorption cross-section, it was not possible to achieve complete light absorption in the PBR during nitrogen limitation. As previously discussed, this was especially illustrated with the culture fed with [NO_3^-] of 1 mM and at an incident PFD of 500 $\mu mol_{h\nu} \cdot m^{-2} \cdot s^{-1}$. It corresponded to the largest MRPA (11,440 $\mu mol_{h\nu} \cdot kg_x^{-1} \cdot s^{-1}$) but with moderate astaxanthin accumulation (3.1 % DW). In contrary, the culture which presented the highest astaxanthin productivity (1.27 ± 0.03 $g \cdot m^{-2} \cdot d^{-1}$) presented a lower MRPA value (8915 $\mu mol_{h\nu} \cdot kg_x^{-1} \cdot s^{-1}$) but the chlorophyll content was found higher and then sufficient (0.45 % DW) to maintain a high photosynthetic capacity and therefore a significant accumulation of astaxanthin (3.9 ± 0.2 % DW). Indeed, when cells are exposed to high MRPA, absorbed light may be dissipated as heat to protect the photosystem rather than being used for biomass or astaxanthin synthesis, and low chlorophyll content can reduce the photosynthetic capacity of cells, which therefore leads to a decrease in growth rate and astaxanthin productivity. Consequently, to optimize astaxanthin production, the light intensity should be optimized and adjusted to avoid loss of light energy by controlling the MRPA in the PBR (≥9000 $\mu mol_{h\nu} \cdot kg_x^{-1} \cdot s^{-1}$), and the level of nitrogen limitation should also be optimized to maintain a sufficient chlorophyll content (≥0.4 % DW) and therefore a significant photosynthetic capacity in the PBR. So large MRPA values were then found to not lead to large astaxanthin concentration per cell nor biomass concentration, resulting then in a smaller astaxanthin productivity. But, as demonstrated in our study, with appropriate nitrate concentration feeding and by controlling the MRPA in the PBR, it was found possible to positively modify cells response and optimize astaxanthin accumulation and productivity.

5. Conclusion

The present study investigated a nitrogen-limited continuous culture protocol with different incident PFD conditions to elucidate the role of those conditions on astaxanthin accumulation in *H. pluvialis* cells. Biomass and astaxanthin productivities were found depended on both rate of photon absorption and nitrate concentration in the feeding medium, with a strong interaction between both due to large change in biomass and pigment concentrations.

A parabolic relationship between MRPA and astaxanthin production rate was obtained, emphasizing existence of an optimal MRPA value to maximize astaxanthin productivity but also that a minimum MRPA (about 8500 ± 500 $\mu mol_{h\nu} \cdot kg_x^{-1} \cdot s^{-1}$) was necessary to trigger large accumulation of astaxanthin in *H. pluvialis* cells. A maximum astaxanthin content and productivity of 3.9 ± 0.2 % DW and 1.27 ± 0.03 $g \cdot m^{-2} \cdot d^{-1}$ respectively were reached for the culture featuring MRPA equal to 8915 $\mu mol_{h\nu} \cdot kg_x^{-1} \cdot s^{-1}$ (with 0.45 % DW in chlorophyll content).

Altogether, we demonstrated that a large quantity of astaxanthin can be produced in a robust and reliable manner in continuous mode under indoor conditions in artificial light PBRs. Our experiment was conducted over almost one year without crash and, moreover, a reversibility of the process and cell response (from green to red stages and vice-versa) was demonstrated. In addition to guarantee a stable production and decrease the number of requested culture systems, the astaxanthin extraction process would certainly be facilitated by the thin-walled cells here obtained, which lack the hard cell wall that characterize the cysts (obtained generally in the two-stage culture system). Obviously, substantial effort is required for further development and scaling up prior to achieving steady operation of the one-step system at a large-scale outdoor condition.

Ethics approval and consent to participate

Not applicable.

Consent for publication

Not applicable.

Funding

This work was funded by the Lebanese University (LU).

Authors' contributions

The manuscript has been read and approved by all named authors, and no other individuals who satisfied the authorship criteria are excluded from the list. The authors further confirm that they have all agreed on the order in which the authors are listed in the manuscript. KS was responsible for conceiving and designing the study, acquiring and analyzing the data, and interpreting the results. KS also wrote the original draft and participated in the final revision. JP and AK were involved in the methodology, conceptualization, investigation, supervision, and data interpretation. HT and AI contributed to the acquisition of funding and provided work supervision. OG et DD were involved in the carotenoids analysis. KS, JP and AK gave final approval for manuscript submission and are responsible for ensuring the integrity of the manuscript as a whole.

CRediT authorship contribution statement

Khadija Samhat: Writing – review & editing, Writing – original draft, Visualization, Validation, Methodology, Investigation, Data curation. **Antoinette Kazbar:** Writing – review & editing, Validation, Supervision. **Hosni Takache:** Writing – review & editing, Validation, Supervision, Funding acquisition. **Olivier Gonçalves:** Writing – review & editing, Validation, Methodology. **Delphine Drouin:** Writing – review & editing, Methodology. **Ali Ismail:** Writing – review & editing, Validation, Resources. **Jeremy Pruvost:** Writing – review & editing, Validation, Supervision, Resources, Project administration, Methodology, Formal analysis, Conceptualization.

Declaration of competing interest

The authors declare that they have no known competing financial interests or personal relationships that could have appeared to influence the work reported in this published article.

Data availability

Main data generated or analyzed during this study are included in this published article.

Acknowledgements

The authors would like to express their gratitude to the Lebanese University (LU) for providing funding for this study, as well as to the GEPEA Laboratory where the experiments were conducted.

References

[1] T. You, S.M. Barnett, Effect of light quality on production of extracellular polysaccharides and growth rate of Porphyridium cruentum, Biochem. Eng. J. 19 (2004) 251–258, https://doi.org/10.1016/j.bej.2004.02.004.
[2] K.H.M. Cardozo, T. Guaratini, M.P. Barros, V.R. Falcão, A.P. Tonon, N.P. Lopes, S. Campos, M.A. Torres, A.O. Souza, P. Colepicolo, E. Pinto, Metabolites from algae with economical impact, Comp. Biochem. Physiol., Part C: Toxicol. Pharmacol. 146 (2007) 60–78, https://doi.org/10.1016/j.cbpc.2006.05.007.
[3] M.A. Borowitzka, High-value products from microalgae—their development and commercialisation, J. Appl. Phycol. 25 (2013) 743–756, https://doi.org/10.1007/s10811-013-9983-9.
[4] M. Koller, A. Muhr, G. Braunegg, Microalgae as versatile cellular factories for valued products, Algal Research 6 (2014) 52–63, https://doi.org/10.1016/j.algal.2014.09.002.
[5] M. Gammone, G. Riccioni, N. D'Orazio, Marine carotenoids against oxidative stress: effects on human health, Mar. Drugs 13 (2015) 6226–6246, https://doi.org/10.3390/md13106226.
[6] B. Capelli, D. Bagchi, G.R. Cysewski, Synthetic astaxanthin is significantly inferior to algal-based astaxanthin as an antioxidant and may not be suitable as a human nutraceutical supplement, Nutrafoods 12 (2013) 145–152, https://doi.org/10.1007/s13749-013-0051-5.
[7] S. Kumar, R. Kumar, A. Diksha, A. Panwar Kumari, Astaxanthin: a super antioxidant from microalgae and its therapeutic potential, J. Basic Microbiol. 62 (2022) 1064–1082, https://doi.org/10.1002/jobm.202100391.
[8] S. Boussiba, W. Bing, J.-P. Yuan, A. Zarka, F. Chen, Changes in pigments profile in the green alga Haeamtococcus pluvialis exposed to environmental stresses, Biotechnol. Lett. 21 (1999) 601–604, https://doi.org/10.1023/A:1005507514694.
[9] R. Ranga, A.R. Sarada, V. Baskaran, G.A. Ravishankar, Identification of carotenoids from green alga *Haematococcus pluvialis* by HPLC and LC-MS (APCI) and their antioxidant properties, J. Microbiol. Biotechnol. 19 (2009) 1333–1341.
[10] B.Y. Zhang, Y.H. Geng, Z.K. Li, H.J. Hu, Y.G. Li, Production of astaxanthin from Haematococcus in open pond by two-stage growth one-step process, Aquaculture 295 (2009) 275–281, https://doi.org/10.1016/j.aquaculture.2009.06.043.
[11] M. Wayama, S. Ota, H. Matsuura, N. Nango, A. Hirata, S. Kawano, Three-dimensional ultrastructural study of oil and astaxanthin accumulation during encystment in the green alga *Haematococcus pluvialis*, PloS One 8 (2013) e53618, https://doi.org/10.1371/journal.pone.0053618.
[12] L. Scibilia, L. Girolomoni, S. Berteotti, A. Alboresi, M. Ballottari, Photosynthetic response to nitrogen starvation and high light in *Haematococcus pluvialis*, Algal Research 12 (2015) 170–181, https://doi.org/10.1016/j.algal.2015.08.024.
[13] H. Sun, B. Liu, X. Lu, K.-W. Cheng, F. Chen, Staged cultivation enhances biomass accumulation in the green growth phase of *Haematococcus pluvialis*, Bioresour. Technol. 233 (2017) 326–331, https://doi.org/10.1016/j.biortech.2017.03.011.
[14] S. Boussiba, A. Vonshak, Astaxanthin accumulation in the green alga *Haematococcus pluvialis*, Plant Cell Physiol. 32 (1991) 1077–1082, https://doi.org/10.1093/oxfordjournals.pcp.a078171.
[15] M. Harker, A.J. Tsavalos, A.J. Young, Factors responsible for astaxanthin formation in the chlorophyte *Haematococcus pluvialis*, Bioresour. Technol. 55 (1996) 207–214, https://doi.org/10.1016/0960-8524(95)00002-X.
[16] M.C. Damiani, C.A. Popovich, D. Constenla, P.I. Leonardi, Lipid analysis in *Haematococcus pluvialis* to assess its potential use as a biodiesel feedstock, Bioresour. Technol. 101 (2010) 3801–3807, https://doi.org/10.1016/j.biortech.2009.12.136.
[17] A.P. Batista, M.C. Nunes, A. Raymundo, L. Gouveia, I. Sousa, F. Cordobés, A. Guerrero, J.M. Franco, Microalgae biomass interaction in biopolymer gelled systems, Food Hydrocoll. 25 (2011) 817–825, https://doi.org/10.1016/j.foodhyd.2010.09.018.
[18] M. Kobayashi, T. Kakizono, N. Nishio, S. Nagai, Y. Kurimura, Y. Tsuji, Antioxidant role of astaxanthin in the green alga *Haematococcus pluvialis*, Appl. Microbiol. Biotechnol. 48 (1997) 351–356, https://doi.org/10.1007/s002530051061.
[19] J. Fábregas, A. Domínguez, M. Regueiro, A. Maseda, A. Otero, Optimization of culture medium for the continuous cultivation of the microalga *Haematococcus pluvialis*, Appl. Microbiol. Biotechnol. 53 (2000) 530–535, https://doi.org/10.1007/s002530051652.
[20] C.D. Kang, J.S. Lee, T.H. Park, S.J. Sim, Complementary limiting factors of astaxanthin synthesis during photoautotrophic induction of *Haematococcus pluvialis*: C/N ratio and light intensity, Appl. Microbiol. Biotechnol. 74 (2007) 987–994, https://doi.org/10.1007/s00253-006-0759-x.
[21] C. Aflalo, Y. Meshulam, A. Zarka, S. Boussiba, On the relative efficiency of two- vs. one-stage production of astaxanthin by the green alga*Haematococcus pluvialis*, Biotechnol. Bioeng. 98 (2007) 300–305, https://doi.org/10.1002/bit.21391.
[22] L. Giannelli, H. Yamada, T. Katsuda, H. Yamaji, Effects of temperature on the astaxanthin productivity and light harvesting characteristics of the green alga *Haematococcus pluvialis*, J. Biosci. Bioeng. 119 (2015) 345–350, https://doi.org/10.1016/j.jbiosc.2014.09.002.
[23] Md.M.R. Shah, Y. Liang, J.J. Cheng, M. Daroch, Astaxanthin-producing green microalga *Haematococcus pluvialis*: from single cell to high value commercial products, Front. Plant Sci. 7 (2016), https://doi.org/10.3389/fpls.2016.00531.
[24] A. Molino, J. Rimauro, P. Casella, A. Cerbone, V. Larocca, S. Chianese, D. Karatza, S. Mehariya, A. Ferraro, E. Hristoforou, D. Musmarra, Extraction of astaxanthin from microalga *Haematococcus pluvialis* in red phase by using generally recognized as safe solvents and accelerated extraction, J. Biotechnol. 283 (2018) 51–61, https://doi.org/10.1016/j.jbiotec.2018.07.010.
[25] S. Pereira, A. Otero, *Haematococcus pluvialis* bioprocess optimization: effect of light quality, temperature and irradiance on growth, pigment content and photosynthetic response, Algal Research 51 (2020) 102027, https://doi.org/10.1016/j.algal.2020.102027.
[26] A. Rizzo, M.E. Ross, A. Norici, B. Jesus, A two-step process for improved biomass production and non-destructive Astaxanthin and carotenoids accumulation in *Haematococcus pluvialis*, Appl. Sci. 12 (2022) 1261, https://doi.org/10.3390/app12031261.
[27] E. Imamoglu, M.C. Dalay, F.V. Sukan, Influences of different stress media and high light intensities on accumulation of astaxanthin in the green alga *Haematococcus pluvialis*, N. Biotechnol. 26 (2009) 199–204, https://doi.org/10.1016/j.nbt.2009.08.007.
[28] E. Del Río, F.G. Acién, M.G. Guerrero, Photoautotrophic production of Astaxanthin by the microalga *Haematococcus pluvialis*, in: O.V. Singh, S.P. Harvey (Eds.), Sustainable Biotechnology: Sources of Renewable Energy, Springer, Netherlands, Dordrecht, 2010, pp. 247–258, https://doi.org/10.1007/978-90-481-3295-9_13.

[29] C. Hagen, K. Grünewald, S. Schmidt, J. Müller, Accumulation of secondary carotenoids in flagellates of *Haematococcus pluvialis* (Chlorophyta) is accompanied by an increase in per unit chlorophyll productivity of photosynthesis, Eur. J. Phycol. 35 (2000) 75–82, https://doi.org/10.1080/09670260010001735651.
[30] C. Hagen, S. Siegmund, W. Braune, Ultrastructural and chemical changes in the cell wall of *Haematococcus pluvialis* (Volvocales, Chlorophyta) during aplanospore formation, Eur. J. Phycol. 37 (2002) 217–226, https://doi.org/10.1017/S0967026202003669.
[31] R. Sarada, R. Vidhyavathi, D. Usha, G.A. Ravishankar, An efficient method for extraction of astaxanthin from green alga *Haematococcus pluvialis*, J. Agric. Food Chem. 54 (2006) 7585–7588, https://doi.org/10.1021/jf060737t.
[32] S. Dong, Y. Huang, R. Zhang, S. Wang, Y. Liu, Four different methods comparison for extraction of astaxanthin from green alga *Haematococcus pluvialis*, Scientific World Journal 2014 (2014) 1–7, https://doi.org/10.1155/2014/694305.
[33] E. Del Río, F.G. Acién, M.C. García-Malea, J. Rivas, E. Molina-Grima, M. G. Guerrero, Efficient one-step production of astaxanthin by the microalga *Haematococcus pluvialis* in continuous culture, Biotechnol. Bioeng. 91 (2005) 808–815, https://doi.org/10.1002/bit.20547.
[34] E. Del Río, F.G. Acién, M.C. García-Malea, J. Rivas, E. Molina-Grima, M. G. Guerrero, Efficiency assessment of the one-step production of astaxanthin by the microalga *Haematococcus pluvialis*, Biotechnol. Bioeng. 100 (2008) 397–402, https://doi.org/10.1002/bit.21770.
[35] M.C. García-Malea, F.G. Acién, E. Del Río, J.M. Fernández, M.C. Cerón, M. G. Guerrero, E. Molina-Grima, Production of astaxanthin by *Haematococcus pluvialis*: taking the one-step system outdoors, Biotechnol. Bioeng. 102 (2009) 651–657, https://doi.org/10.1002/bit.22076.
[36] J. Wang, D. Han, M.R. Sommerfeld, C. Lu, Q. Hu, Effect of initial biomass density on growth and astaxanthin production of *Haematococcus pluvialis* in an outdoor photobioreactor, Journal of Applied Phycology 25 (2013) 253–260, https://doi.org/10.1007/s10811-012-9859-4.
[37] W. Zhang, X. Zhou, Y. Zhang, P. Cheng, R. Ma, W. Cheng, H. Chu, Enhancing astaxanthin accumulation in *Haematococcus pluvialis* by coupled light intensity and nitrogen starvation in column photobioreactors, J. Microbiol. Biotechnol. 28 (2018) 2019–2028, https://doi.org/10.4014/jmb.1807.07008.
[38] M.C. Cerón, M.C. García-Malea, J. Rivas, F.G. Acien, J.M. Fernandez, E. Del Río, M. G. Guerrero, E. Molina, Antioxidant activity of *Haematococcus pluvialis* cells grown in continuous culture as a function of their carotenoid and fatty acid content, Appl. Microbiol. Biotechnol. 74 (2007) 1112–1119, https://doi.org/10.1007/s00253-006-0743-5.
[39] G. Van Vooren, F. Le Grand, J. Legrand, S. Cuiné, G. Peltier, J. Pruvost, Investigation of fatty acids accumulation in Nannochloropsis oculata for biodiesel application, Bioresour. Technol. 124 (2012) 421–432, https://doi.org/10.1016/j.biortech.2012.08.009.
[40] R. Kandilian, J. Pruvost, J. Legrand, L. Pilon, Influence of light absorption rate by Nannochloropsis oculata on triglyceride production during nitrogen starvation, Bioresour. Technol. 163 (2014) 308–319, https://doi.org/10.1016/j.biortech.2014.04.045.
[41] R. Kandilian, A. Taleb, V. Heredia, G. Cogne, J. Pruvost, Effect of light absorption rate and nitrate concentration on TAG accumulation and productivity of Parachlorella kessleri cultures grown in chemostat mode, Algal Res. 39 (2019) 101442, https://doi.org/10.1016/j.algal.2019.101442.
[42] V. Heredia, L. Marchal, O. Gonçalves, J. Pruvost, Optimization of continuous TAG production by *Nannochloropsis gaditana* in solar-nitrogen-limited culture, Biotech & Bioengineering 119 (2022) 1808–1819, https://doi.org/10.1002/bit.28097.
[43] K. Samhat, A. Kazbar, H. Takache, A. Ismail, J. Pruvost, Influence of light absorption rate on the astaxanthin production by the microalga *Haematococcus pluvialis* during nitrogen starvation, Bioresour. Bioprocess. 10 (2023) 78, https://doi.org/10.1186/s40643-023-00700-0.
[44] J.F. Cornet, C.G. Dussap, P. Cluzel, G. Dubertret, A structured model for simulation of cultures of the cyanobacteriumSpirulina platensis in photobioreactors: II. Identification of kinetic parameters under light and mineral limitations, Biotechnol. Bioeng. 40 (1992) 826–834, https://doi.org/10.1002/bit.260400710.
[45] E.M. Grima, F.G. Camacho, J.A.S. Pérez, J.M.F. Sevilla, F.G.A. Fernández, A. C. Gómez, A mathematical model of microalgal growth in light-limited chemostat culture, J. Chem. Technol. Biotechnol. 61 (1994) 167–173, https://doi.org/10.1002/jctb.280610212.
[46] J.-F. Cornet, C.-G. Dussap, A simple and reliable formula for assessment of maximum volumetric productivities in photobioreactors, Biotechnol Progress 25 (2009) 424–435, https://doi.org/10.1002/btpr.138.
[47] H. Takache, G. Christophe, J.-F. Cornet, J. Pruvost, Experimental and theoretical assessment of maximum productivities for the microalgae *Chlamydomonas reinhardtii* in two different geometries of photobioreactors, Biotechnol Progress (2009), https://doi.org/10.1002/btpr.356.
[48] H. Takache, J. Pruvost, J.-F. Cornet, Kinetic modeling of the photosynthetic growth of Chlamydomonas reinhardtii in a photobioreactor, Biotechnol. Prog. 28 (2012) 681–692, https://doi.org/10.1002/btpr.1545.
[49] Q. Béchet, A. Shilton, B. Guieysse, Modeling the effects of light and temperature on algae growth: state of the art and critical assessment for productivity prediction during outdoor cultivation, Biotechnol. Adv. 31 (2013) 1648–1663, https://doi.org/10.1016/j.biotechadv.2013.08.014.
[50] A.E. Cassano, C.A. Martin, R.J. Brandi, O.M. Alfano, Photoreactor analysis and design: fundamentals and applications, Ind. Eng. Chem. Res. 34 (1995) 2155–2201, https://doi.org/10.1021/ie00046a001.
[51] J. Pruvost, J.-F. Cornet, Knowledge models for the engineering and optimization of photobioreactors, in: C. Posten, C. Walter (Eds.), Microalgal Biotechnology: Potential and Production, De Gruyter, 2012, pp. 181–224. https://hal.archives-ouvertes.fr/hal-02539915.
[52] M. Jonasz, G. Fournier, Light Scattering by Particles in Water: Theoretical and Experimental Foundations, 1st ed, Elsevier/Academic Press, Amsterdam, 2007. https://search.ebscohost.com/login.aspx?direct=true&scope=site&db=nlebk&db=nlabk&AN=203339.
[53] L. Pottier, J. Pruvost, J. Deremetz, J.-F. Cornet, J. Legrand, C.G. Dussap, A fully predictive model for one-dimensional light attenuation by Chlamydomonas reinhardtii in a torus photobioreactor, Biotechnol. Bioeng. 91 (2005) 569–582, https://doi.org/10.1002/bit.20475.
[54] E. Lee, J. Pruvost, X. He, R. Munipalli, L. Pilon, Design tool and guidelines for outdoor photobioreactors, Chem. Eng. Sci. 106 (2014) 18–29, https://doi.org/10.1016/j.ces.2013.11.014.
[55] R. Kandilian, A. Soulies, J. Pruvost, B. Rousseau, J. Legrand, L. Pilon, Simple method for measuring the spectral absorption cross-section of microalgae, Chem. Eng. Sci. 146 (2016) 357–368, https://doi.org/10.1016/j.ces.2016.02.039.
[56] F.R. Ferrel Ballestas, M. Titica, J. Legrand, L. Pilon, G. Cogne, Prediction of the radiation characteristics and the light absorption rate of Chlamydomonas reinhardtii cultivated under a progressive nitrogen starvation and accumulating carbon reserves, J. Quant. Spectrosc. Radiat. Transf. 309 (2023) 108708, https://doi.org/10.1016/j.jqsrt.2023.108708.
[57] H.W. Nichols, H.C. Bold, Trichosarcina polymorpha Gen. et Sp. Nov, J. Phycol. 1 (1965) 34–38, https://doi.org/10.1111/j.1529-8817.1965.tb04552.x.
[58] J. Pruvost, G. Van Vooren, G. Cogne, J. Legrand, Investigation of biomass and lipids production with Neochloris oleoabundans in photobioreactor, Bioresour. Technol. 100 (2009) 5988–5995, https://doi.org/10.1016/j.biortech.2009.06.004.
[59] J. Pruvost, J.-F. Cornet, J. Legrand, Hydrodynamics influence on light conversion in photobioreactors: an energetically consistent analysis, Chem. Eng. Sci. 63 (2008) 3679–3694, https://doi.org/10.1016/j.ces.2008.04.026.
[60] V. Heredia, O. Gonçalves, L. Marchal, J. Pruvost, Producing energy-rich microalgae biomass for liquid biofuels: influence of strain selection and culture conditions, Energies 14 (2021) 1246, https://doi.org/10.3390/en14051246.
[61] N. Qiu, X. Wang, F. Zhou, A new method for fast extraction and determination of chlorophylls in natural water, Zeitschrift Für Naturforschung C 73 (2018) 77–86, https://doi.org/10.1515/znc-2017-0157.
[62] J.D.H. Strickland, T.R. Parsons, A practical handbook of seawater analysisBulletin of Fisheries 167, Research Board of Canada, 1968, pp. 1–311.
[63] S. Boussiba, L. Fan, A. Vonshak, [36] Enhancement and determination of astaxanthin accumulation in green alga *Haematococcus pluvialis*, in: Methods in Enzymology, Elsevier, 1992, pp. 386–391, https://doi.org/10.1016/0076-6879(92)13140-S.
[64] F. Su, H. Xu, N. Yang, W. Liu, J. Liu, Hydrolytic efficiency and isomerization during de-esterification of natural astaxanthin esters by saponification and enzymolysis, Electron. J. Biotechnol. 34 (2018) 37–42, https://doi.org/10.1016/j.ejbt.2018.05.002.
[65] M. Olaizola, Commercial production of astaxanthin from Haematococcus pluvialis using 25,000-liter outdoor photobioreactors, J. Appl. Phycol. 12 (2000) 499–506, https://doi.org/10.1023/A:1008159127672.
[66] L. Zhang, F. Su, C. Zhang, F. Gong, J. Liu, Changes of photosynthetic behaviors and photoprotection during cell transformation and astaxanthin accumulation in *Haematococcus pluvialis* grown outdoors in tubular Photobioreactors, IJMS 18 (2016) 33, https://doi.org/10.3390/ijms18010033.
[67] C. Hu, D. Cui, X. Sun, J. Shi, N. Xu, Primary metabolism is associated with the astaxanthin biosynthesis in the green algae *Haematococcus pluvialis* under light stress, Algal Research 46 (2020) 101768, https://doi.org/10.1016/j.algal.2019.101768.